Dalton Transactions

PAPER

View Article Online
View Journal | View Issue

Cite this: *Dalton Trans.*, 2015, **44**, 9551

Large and negative magnetic anisotropy in pentacoordinate mononuclear Ni(II) Schiff base complexes†

Ivan Nemec,[a] Radovan Herchel,[a] Ingrid Svoboda,[b] Roman Boča[c] and Zdeněk Trávníček*[a]

Received 10th February 2015,
Accepted 9th April 2015

DOI: 10.1039/c5dt00600g

www.rsc.org/dalton

A series of pentacoordinate Ni(II) complexes of the general formula [Ni(L5)] (**1–6**) with various pentadentate Schiff base ligands H_2L5 (originating in a condensation of aromatic *ortho*-hydroxy-aldehydes and aliphatic triamines) was synthesized and characterized by X-ray structure analysis and magnetometry. The alternations of substituents on the H_2L parent ligand resulted in the complexes with the geometry varying between the square-pyramid and trigonal-bipyramid. In the compounds whose chromophore geometry is closer to a trigonal-bipyramid, a large and negative uniaxial anisotropy (D = −64 cm^{-1}) was identified. Moreover, the simple linear expression for the axial zero-field splitting (ZFS) parameter, D/cm^{-1} = 32.7(4.8) − 151(10)τ, was proposed, where τ (in degrees) stands for the Addison parameter. The results of magnetic analysis were also supported by *ab initio* CASSCF/NEVPT2 calculations of the ZFS splitting parameters D and E, and g tensors. Despite large and negative D-values of the reported compounds, slow relaxation of magnetization was not observed either in zero or non-zero static magnetic field, thus no single-molecule magnetic behaviour was detected.

Introduction

The potential industrial utilization of the molecular materials exhibiting slow relaxation of magnetization (SRM), single-molecule magnets (SMM), has driven the research of magnetic anisotropy[1] of coordination compounds in the last two decades. The relation of magnetic anisotropy (expressed by the axial (D) and rhombic (E) zero-field splitting parameters) to the spin-reversal barrier height (U_{eff}) plays a crucial role in potential application of compounds showing SRM phenomenon.

At the very beginning of the SMM research, the attention was focused mainly on polynuclear coordination compounds. However, in these it is difficult to tune rationally the magnetic exchange and anisotropy in order to increase U_{eff}. Lately, it has been shown that magnetic anisotropy is the key component in this effort,[2] which was further proven by the extensive work on the lanthanide mononuclear SMM (single-ion magnets, SIM)[3] and the discovery of SIM for the first-row transition metals such as Mn(III),[4] Fe(I),[5] Fe(II),[6] Fe(III),[7] Co(II),[8] and Ni(I).[9] In these systems structural distortions along with spin–orbit coupling induce large magnetic anisotropy and subsequently, the SIM behaviour. However, the rational design of SIM is still far from being routine.

In order to explore the molecular structure–magnetic anisotropy relationship in the M(II) coordination compounds, several magneto-structural D-correlations for hexacoordinate Ni(II) and Co(II) complexes have been outlined.[10] However, to the best of our knowledge, these correlations have not covered the pentacoordinate Ni(II) complexes yet. Only very recently the proposition of such a correlation for pentacoordinate Co(II) complexes with various coordination donor sets (*i.e.* N_3X_2, N_3O_2, X = halide anion) has been reported.[11] While hexacoordinate Ni(II) compounds adopt relatively large D values, from −10 to +10 cm^{-1}, magnetic anisotropy is much more enhanced in pentacoordinate Ni(II) complexes with a trigonal-bipyramid geometry of the chromophore for which very large and negative values of the D-parameters, ranging from −120 to −200 cm^{-1}, have been found.[12] This is due to the orbitally degenerate ground term ^3E in the D_{3h} symmetry (trigonal-bipyramid, abbr. TB) of the coordination polyhedron in the case of Ni(II) compounds.[13] At this point it must be noted that

[a]*Regional Centre of Advanced Technologies and Materials, Department of Inorganic Chemistry, Faculty of Science, Palacký University, Tř. 17. listopadu 12, CZ-77146 Olomouc, Czech Republic. E-mail: zdenek.travnicek@upol.cz*
[b]*Materials Science, Darmstadt University of Technology, D-64287 Darmstadt, Germany. E-mail: svoboda@tu-darmstadt.de*
[c]*Department of Chemistry, FPV, University of SS Cyril and Methodius, 91701 Trnava, Slovakia. E-mail: roman.boca@stuba.sk*

† Electronic supplementary information (ESI) available. CCDC 1047940–1047943. For ESI and crystallographic data in CIF or other electronic format see DOI: 10.1039/c5dt00600g

no Ni(II) SIM has been reported for Ni(II) pentacoordinate compounds so far. Hence it is clear that this topic deserves much more scientific effort as TB compounds of Ni(II) might be appropriate candidates for the observation of SRM and thus the SIM behaviour. In the theoretical work of Pavlovic *et al.*[13] a strategy for obtaining such compounds was proposed as follows: (a) preparation of the compounds with the TB geometry (or the geometry very close to TB); (b) use of the robust and polydentate ligands, which might prevent Jahn–Teller (JT) distortion present in TB Ni(II) compounds (as a consequence of the JT effect, symmetry lowering causes removal of the orbital degeneracy reflecting itself in much lower *D*-values); and (c) utilization of the ligands with weak ligand field strengths.

This motivated us to prepare new Ni(II) pentacoordinate complexes involving pentadentate Schiff base ligands, because they fulfil several of the above mentioned criteria (*i.e.* relatively robust ligands, weak ligand field) for the preparation of pentacoordinate Ni(II) complexes with a large and negative *D* parameter.

The pentadentate Schiff base ligands originating in a condensation of aromatic 2-hydroxy aldehydes and aliphatic triamines (Scheme 1) can be prepared easily and therefore, they are suitable for a systematic study involving modulation of the complex properties *via* ligand substitutions. Most importantly, in combination with Ni(II), Co(II) and Fe(II) salts, these ligands form pentacoordinate complexes of the general composition $[M^{II}(L5)]$.[14] The Ni(II) compounds of this type are further abbreviated as [Ni(L5)] in this work.

In this work we report on the crystal structure and magnetic properties of Ni(II) complexes of the aforementioned general composition, namely complexes [Ni(L5A)] (**1**), [Ni(L5B)] (**2**), and [Ni(L5C)] (**3**). Furthermore, magnetic properties of previously reported (structural and spectroscopic studies only) compounds [Ni(L5D)][15] (**4**), [Ni(L5E)][16] (**5**), and [Ni(L5F)][17] (**6**) were measured, analysed and included in this study (Scheme 1). The magnetic data (temperature and field dependence of the magnetisation) were analysed using the spin-Hamiltonian formalism that covers the zero-field splitting (ZFS) terms (both axial and rhombic). Such approach provided a reliable set of ZFS parameters which were correlated with the crystal structure of the presented compounds. Furthermore, the *ab initio* calculations on the molecular structures were employed to support the magnetic analysis by calculating ZFS and *g* tensors, which helped in revealing the relationship between the chromophore geometry and magnetic anisotropy.

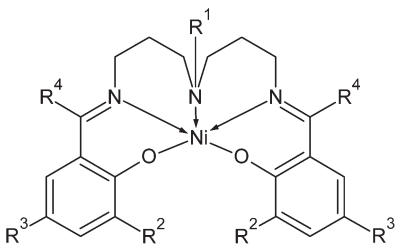

Scheme 1 Schematic representations of pentacoordinate Ni(II) complexes presented in this work: **1**, [Ni(L5A)] ($R^1 = R^3 = -CH_3$, $R^2 = -C(CH_3)_3$, R^4 = H); **2**, [Ni(L5B)], ($R^1 = -CH_3$, $R^2 = R^4$ = H, R^3 = Br); **3**, [Ni-(L5C)], ($R^1 = -CH_3$, $R^2 = R^4$ = H, R^3 = I); **4**, [Ni(L5D)], ($R^1 = -CH_3$, $R^2 = R^3 = -C(CH_3)_3$, R^4 = H); **5**, [Ni(L5E)], ($R^1 = -CH_3$, $R^2 = R^3 = R^4$ = H); **6**, [Ni-(L5F)] ($R^1 = R^3 = R^3$ = H, $R^4 = -CH_3$).

Results

Synthesis and crystal structure

The preparation of the compounds under study is rather simple and it is based on the first report on $[Ni^{II}(L5)]$-type compounds by Seleborg *et al.*[18] In the first step, the bis(salicylaldehydato)nickel(II) complex is prepared by the reaction of nickel(II) acetate tetrahydrate and the corresponding derivative of salicylaldehyde in methanol. Then, the corresponding aliphatic triamine (bis(3-aminopropyl)amine or 3,3′-diamino-*N*-methyldipropylamine in this case) is added to the reaction mixture which immediately turns green. Single-crystals were obtained by slow evaporation of the mother liquor (**1**) or by recrystallization of the microcrystalline product (for details see the Experimental section).

The crystal structures were determined for three new compounds **1–3**, and the structure of **5** was redetermined, because Cambridge Crystallographic Database (CSD)-deposited[19] structural data was of low quality. For compounds **4** and **6** the structural data were retrieved from CSD. The selected bond lengths and structural parameters are summarized in Table 1; crystal data and structural refinements for compounds **1**, **2**, **3** and **5** are listed in Table 2.

Structural features are very similar for all the reported compounds in this study (Fig. 1). The doubly deprotonated ($L5^{2-}$) pentadentate ligands provide the $\{N_3O_2\}$ donor set by one amine (N_{am}) and two imino nitrogen atoms (N_{im}) and two phenolato oxygen atoms (oxygen atoms are in the *cis* position). The longest bond lengths within the chromophore are found for Ni–N_{am} bonds ranging from 2.05 to 2.10 Å. The Ni–N_{im} bonds are a bit shorter (1.99–2.03 Å) and the Ni–O bonds are the shortest (1.95–2.00 Å). It can be summarised that the bond lengths in the studied [Ni(L5)] derivatives are very similar in all the reported compounds in this study (Table 1).

The chromophores in **1–6** adopt shapes intermediate between square-pyramid (SP) and trigonal-bipyramid (TB). The

Table 1 Selected bond lengths (Å) and structural parameters τ and α

	Ni–N_{am}	Ni–N_{im} [a]	Ni–O[a]	τ/°	α/°
1	2.087(3)	2.004	1.983	0.52	110.6
2	2.088(3)	2.005	1.980	0.62	131.3
3	2.086(4)	2.003	1.974	0.62	132.8
4	2.099	2.009	1.997	0.47	138.0
5	2.094(4)	2.015	1.973	0.60	102.0
6	2.050(1)	2.039	1.976	0.26	80.6

[a] Average value calculated from two values. For definition of angles τ and α see text.

Table 2 Crystal data and structure refinements for complexes **1**, **2**, **3** and **5**

	1	2	3	5
Formula	$C_{31}H_{45}N_3NiO_2$	$C_{21}H_{23}Br_2N_3NiO_2$	$C_{21}H_{23}I_2N_3NiO_2$	$C_{21}H_{25}N_3NiO_2$
Formula weight	550.41	567.95	661.94	410.15
Crystal system	Monoclinic	Monoclinic	Monoclinic	Monoclinic
Space group	$P2_1/c$	$P2_1/c$	$P2_1/c$	$P2_1/c$
Temperature/K	303	150	150	298
a/Å	13.6320(10)	10.1636(7)	10.3149(6)	6.9490(8)
b/Å	17.9180(10)	26.5733(13)	27.6223(12)	14.037(2)
c/Å	12.6470(10)	8.5995(7)	8.4460(5)	20.113(5)
α/°	90	90	90	90
β/°	99.475(7)	113.486(9)	113.807(7)	92.008(13)
γ/°	90	90	90	90
V/Å^3	3047.0(4)	2130.1(2)	2201.7(3)	1960.7(6)
Z, ρ_{calc}/g cm^{-3}	4, 1.200	4, 1.771	4, 1.997	4, 1.389
μ/mm^{-1}	0.667	4.685	3.708	1.010
Final R indices, R_1 [a]	0.0453	0.0283	0.0279	0.0552
$[I > 2\sigma(I)]$, wR_2 [b]	0.0988	0.0553	0.0615	0.1235
R indices all data R_1 [a]	0.0946	0.0464	0.0362	0.1075
wR_2 [b]	0.1132	0.0577	0.0634	0.1378
CCDC number	1047940	1047941	1047942	1047943

[a] $R_1 = \sum(|F_o| - |F_c|)/\sum|F_o|$. [b] $wR^2 = \{\sum[w(F_o^2 - F_c^2)^2]/\sum[w(F_o^2)^2]\}^{1/2}$.

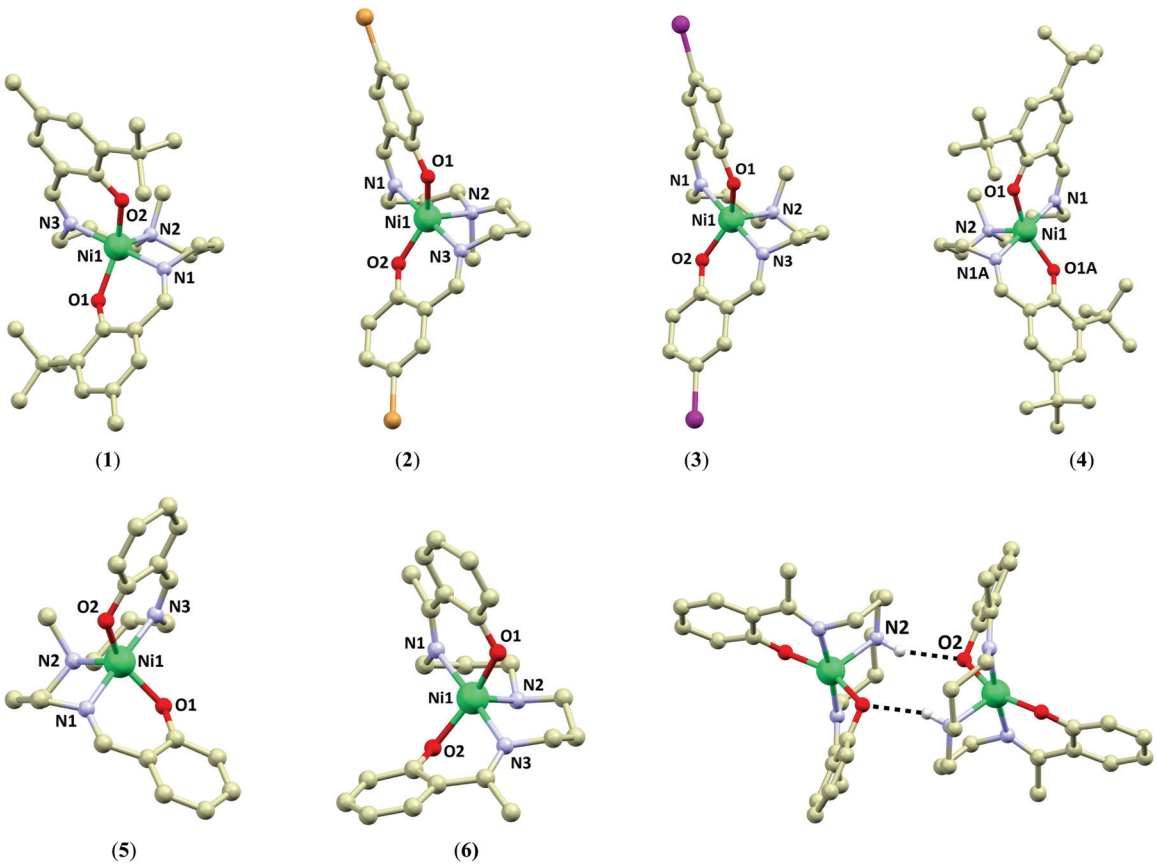

Fig. 1 Molecular structures of compounds **1–6** (the structural data of compounds **4**[15] and **6**[17] were retrieved from Cambridge Structural Database, CSD). *Bottom-right*: A view on the supramolecular dimer held together by N–H···O hydrogen bonding (dashed black lines) in **6**. Hydrogen atoms are omitted for clarity, except for those involved in hydrogen bonding. Selected bond lengths (in Å): **1**, Ni1–N2 = 2.087(3), Ni1–N1 = 2.005(2), Ni1-N3 = 2.002(3), Ni1–O2 = 1.968(2), Ni1–O1 = 1.998(2); **2**, Ni1–N1 = 1.998(3), Ni1–N2 = 2.087(3), Ni1–N3 = 2.013(2), Ni1–O1 = 1.966(2), Ni1-O2 = 1.994(2); **3**, Ni1–N1 = 2.006(3), Ni1–N2 = 2.085(3), Ni1–N3 = 2.000(3), Ni1–O1 = 1.983(3), Ni1–O2 = 1.965(3); **4**, Ni1–N1 = 2.009, Ni1–N2 = 2.099, Ni1–O1 = 1.997; **5**, Ni1–N1 = 2.017(4), Ni1–N2 = 2.094(4), Ni1–N3 = 2.013(4), Ni1–O1 = 1.974(3), Ni1–O2 = 1.971(3); **6**, Ni1–N1 = 2.033(1), Ni1–N2 = 2.050(1), Ni1–N3 = 2.044(1), Ni1–O1 = 1.950(1), Ni1–O2 = 2.002(1).

characterization of these two possible limiting pentacoordinate geometries is well established by the Addison parameter τ[20] which adopts zero value for the purely SP geometry and τ = 1 for the TB geometry. In the present series the τ parameters span a relatively large range (Table 1) with the lowest value found for **6** (τ = 0.26) and the largest ones found for **2** and **3** (τ = 0.62).

The group of the $L5^{2-}$ ligands is well-known for their structural flexibility and this fact can influence the geometry of the chromophore.[21] In order to examine a possible relationship between the shape of the $L5^{2-}$ ligand and τ parameter, the parameter α (the dihedral angle between the least squares planes of the aromatic rings) was used.

From the obtained α values one can see that there is no apparent correlation between these two parameters; however, the lowest value of α is found for compound **6** exhibiting also the lowest τ value. Similar to **6**, the compound containing the L5-type ligand with comparable τ and α parameters (α = 67.1, τ = 0.25) can be retrieved from the CCDC – [Ni(L5G)] (where LG^{2-} = *N*,*N*′-bis((2-hydroxy-5-methylphenyl)(phenyl)methylene)-4-azaheptane-1,7-diamine). Interestingly the ligands in both compounds (**6** and [Ni(L5G)]) arise from condensation of ketones with amines (1-(2-hydroxyphenyl)ethanone in **6**, and (2-hydroxy-5-methylphenyl)(phenyl)methanone in [Ni(L5G)]). This indicates that the use of the ketones in preparing [Ni(L5)] results in pentacoordinate complexes with the chromophore geometry close to SP.

In compounds **1–5**, the non-covalent interactions are of C–H···O/C or C–H···π type and they are of negligible strength. In **6**, the N–H···O hydrogen bonds between the amine group and phenolato oxygen atom stabilize a centrosymmetric supramolecular dimer (Fig. 1). The donor–acceptor distance is relatively large: *d*(N···O) = 3.059(2) Å. The face-to-face π–π stacking is absent in **1–6**.

Magnetic properties

The temperature dependence of the effective magnetic moment (μ_{eff}) and the field dependence of the magnetization (M_{mol}) of all the investigated compounds are shown in Fig. 2. The spin-only value for Ni(II) complexes is μ_{eff} = 2.83μ_B and it is apparent from Fig. 2 that μ_{eff} is much higher at room temperature: 3.0–3.2μ_B for **1–6**. Thus, significant contribution of angular momentum (and g > 2.0) to overall magnetic properties must be considered. The effective magnetic moment for **1–6** stays almost constant at 70 K; it drops down to 1.7–1.9μ_B at T = 1.9 K. The isothermal magnetizations measured at 2.0 and 5.0 K showed large deviation from the Brillouin function. These features confirm sizable values of the ZFS parameters and consequently large magnetic anisotropy.

In magnetic data analysis the following spin Hamiltonian was considered,

$$\hat{H} = D(\hat{S}_z^2 - \hat{S}^2/3) + E(\hat{S}_x^2 - \hat{S}_y^2) + \mu_B B_a g \hat{S}_a \quad (1)$$

where D and E are the single-ion axial, and rhombic ZFS parameters, respectively. The last part is the spin-Zeeman term, in which a direction of the magnetic field is defined as $B_a = B(\sin\theta\cos\varphi,\ \sin\theta\sin\varphi,\ \cos\theta)$ with the help of the polar coordinates. Then, the molar magnetization in the a-th direction of the magnetization can be numerically calculated as,

$$M_a = RT\frac{\partial \ln Z}{\partial B_a} \quad (2)$$

where Z is the partition function. Finally, the averaged molar magnetization of the powder sample was calculated as an integral average

$$M_{mol} = 1/4\pi \int_0^{2\pi}\int_0^{\pi} M_a \sin\theta d\theta d\varphi \quad (3)$$

In order to determine the spin Hamiltonian parameters, both temperature and field dependent magnetization data were fitted simultaneously (Fig. 2). Furthermore, the standard deviations of the varied parameters were calculated with the 95% probability confidence limits.[22] The final set of magnetic parameters is listed in Table 3. In all the cases, the *D*-parameter was found negative, meaning that complexes **1–6** possess an easy-axis of magnetization. The largest *D*-parameter was found for **2** (D = −64.0 cm^{-1}), while the smallest D and largest rhombicity was found for **6** (D = −12.7 cm^{-1}, E/D = 0.18). This stimulated the measurement of the AC susceptibility in zero and in applied static magnetic fields; however, no out-of-phase susceptibility signal was detected for herein reported compounds **1–5**.

Ab initio calculations

In order to support the experimental results, we utilized the contemporary *ab initio* theoretical method based on multireference state average complete active space (SA-CASSCF) wavefunctions complemented by N-electron valence state perturbation theory (NEVPT) with CAS(8,5) active space. This enabled computing of the *D*- and *g*-tensors for studied compounds **1–6**.

The results of calculations are summarized in Table 3. Generally, the *ab initio* calculations confirm large and negative *D*-parameters ranging from −41.7 to −63.2 cm^{-1} and also relatively small rhombicity (E/D < 0.07) in **1–5**. In **6**, the considerably lower axial ZFS parameter was found, D = −25.3 cm^{-1}, with a much higher rhombicity, E/D = 0.17. The calculated D and E/D values agree with those extracted for the experimental data for **1–4**; however, in **5** and **6** the discrepancy between the calculation and experiment is larger (Table 3). The contributions of excited states to the ZFS terms are tabulated in Tables S1–S6 (see ESI†). Furthermore, the energy levels of ligand field multiplets for the studied compounds are listed in Table S7 (ESI†) showing that first excited multiplet is at least ~4000 cm^{-1} above the ground state triplet, which justifies use of the spin Hamiltonian to analyse their magnetic properties.

The axes of the calculated ZFS and *g*-tensors together with the molecular structures are visualized in Fig. 3. In all the

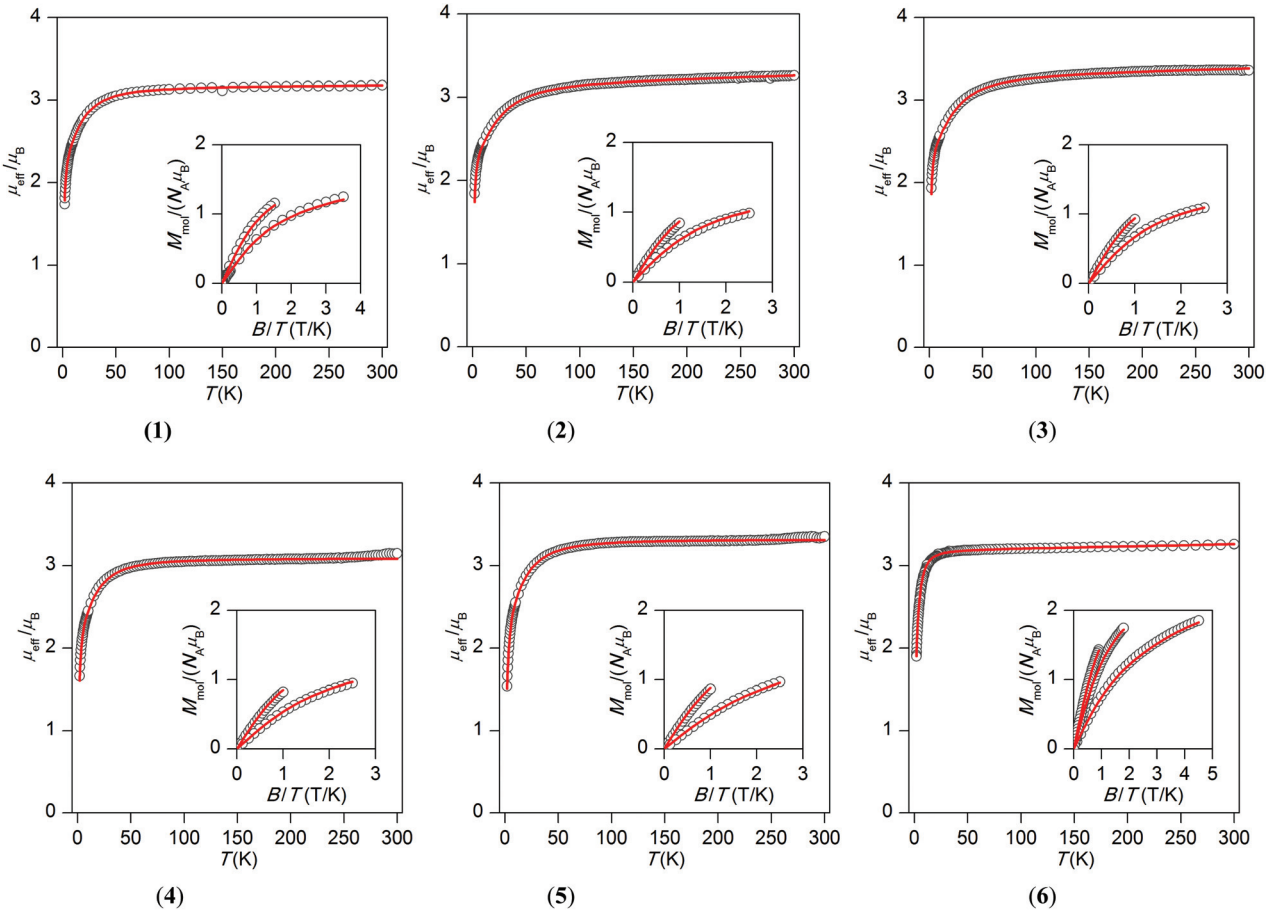

Fig. 2 Magnetic properties of compounds **1–6**. Each plot shows the temperature dependence of the effective magnetic moment and in the inset the reduced isothermal magnetizations measured at T = 2.0 and 5.0 K or eventually also at 10 K (**6**) are given. Experimental data – empty symbols, full lines – the best fit calculated with D = −45(3) cm^{-1}, E/D = 0.046(2), g = 2.23(1) and χ_{TIP} = 0.9(1.0) × 10^{-9} m^3 mol^{-1} for **1**, D = −64(4) cm^{-1}, E/D = 0.034(2), g = 2.24(1) and χ_{TIP} = 3.5(8) × 10^{-9} m^3 mol^{-1} for **2**, D = −60(3) cm^{-1}, E/D = 0.033(1), g = 2.33(1) and χ_{TIP} = 3.4(7) × 10^{-9} m^3 mol^{-1} for **3**, D = −45(2) cm^{-1}, E/D = 0.058(3), g = 2.183(3) for **4**, D = −49(2) cm^{-1}, E/D = 0.073(3), g = 2.345(3) for **5**, D = −12.7(3) cm^{-1}, E/D = 0.183(7), g = 2.251(4) and χ_{TIP} = 2.6(5) × 10^{-9} m^3 mol^{-1} for **6**.

Table 3 Spin Hamiltonian parameters of **1–8** derived from magnetic data and from CASSCF/NEVPT2/ZORA/def2-TZVP(-f) calculations

	Magnetic data analysis			*Ab initio* calculations		
	D/cm^{-1}	E/D	g	D/cm^{-1}	E/D	g_1, g_2, g_3
1	−45(3)	0.046(2)	2.23(1)	−49.1	0.045	2.151, 2.195, 2.512
2	−64(4)	0.034(2)	2.24(1)	−52.6	0.044	2.147, 2.191, 2.531
3	−60(3)	0.033(1)	2.33(1)	−52.0	0.047	2.145, 2.191, 2.526
4	−45(2)	0.058(2)	2.183(4)	−41.7	0.068	2.154, 2.207, 2.472
5	−49(2)	0.073(3)	2.345(3)	−63.2	0.037	2.145, 2.188, 2.596
6	−12.7(3)	0.183(7)	2.251(4)	−25.3	0.169	2.155, 2.227, 2.370
7[a]	+15.9		2.17	+22.7	0.33	2.134, 2.261, 2.356
8 (Ni1)[a]	+16.7	0.0/0.036	2.18	+20.0	0.063	2.134, 2.287, 2.293
8 (Ni2)[a]				+19.0	0.097	2.136, 2.281, 2.289

[a] The experimental data from magnetic data analysis for compounds **7** and **8** are adopted from ref. 20.

cases, the g-tensors and ZFS-tensor axes almost coincide, and under conditions that ZFS-tensor defines coordination axes X, Y and Z the following relationships hold true for g-components: $g_x = g_2$, $g_y = g_1$, and $g_z = g_3$. In spite of the fact that the calculated axes of the ZFS tensors and donor–acceptor bonds do not tally perfectly, we can roughly identify the Z-axis of the

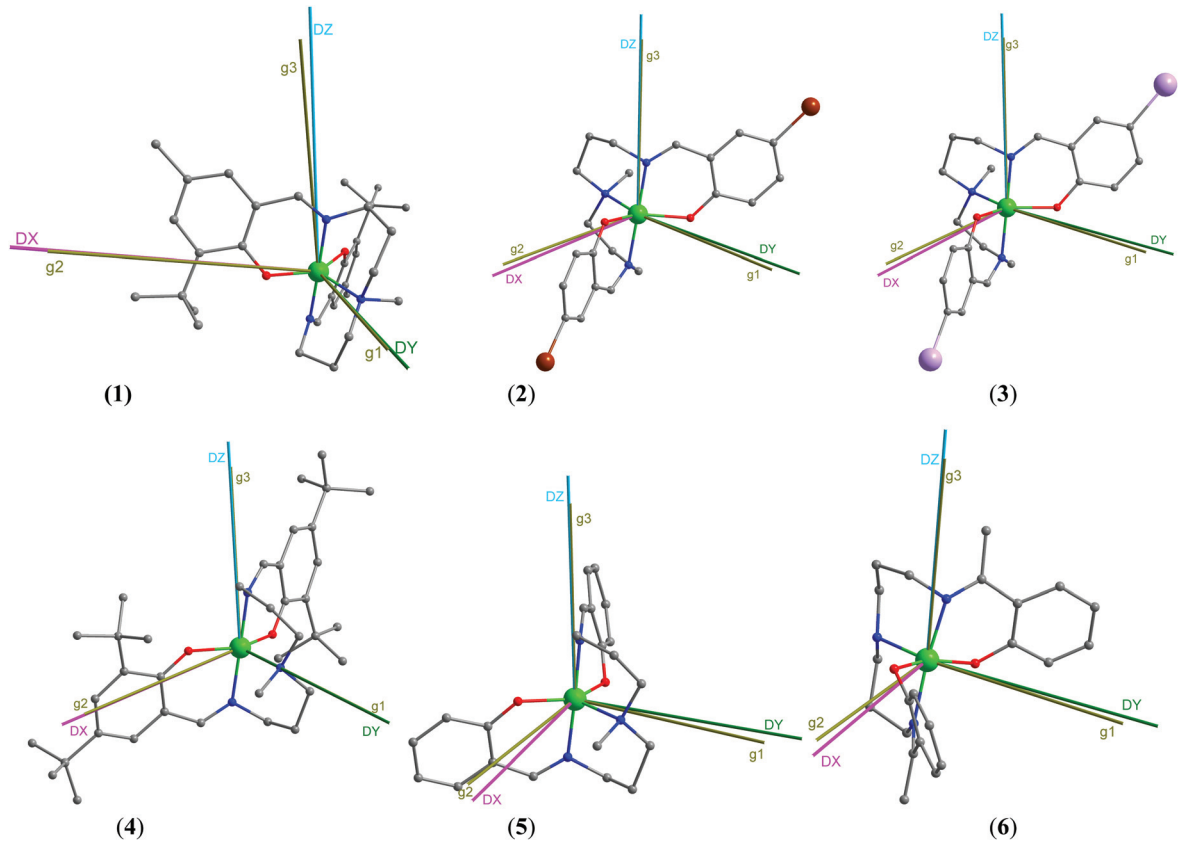

Fig. 3 The CASSCF/NEVPT2 principal axes of ZFS tensors labelled as DX, DY, DZ, and axes of *g* tensors labelled as *g1*, *g2*, *g3* visualized together with the molecular structures of compounds **1–6**. The hydrogen atoms were omitted for clarity.

ZFS tensors in **1–6** with the Ni–N_{im} bonds, while the other two axes *X* and *Y* lay along the Ni–O, and Ni–N_{am} bonds, respectively. With the aim to find the magneto-structural correlation, the axial ZFS parameter *D* was plotted as a function of the geometrical parameter τ. Two previously reported compounds (with related ligands and similar chromophore, $\{NiN_4O\}$),[23] [Ni(L3A)(L2)](ClO_4) (**7**) and [Ni(L3B)(L2)](ClO_4) (**8**) where (L3A = 2-[(1*E*)-*N*-(2-amino-2-methylpropyl)ethanimidoyl]-phenol, L3B = 2-[(1*E*)-*N*-(2-amino-2-aminopropyl)-ethanimidoyl]phenol, L2 = 6,6′-dimethyl-2,2′bipyridine), were also involved in the analysis in order to enlarge the dataset; they possess τ(**7**) = 0.09 and τ(**8**_Ni1) = 0.13, τ(**8**_Ni2) = 0.086. Furthermore, for these compounds the same *ab initio* calculations at the CASSCF/NEVPT2 level of theory were performed as for compounds **1–6** and the results are listed in Table 3. Then, both experimental and calculated datasets resemble a linear dependence of *D vs.* τ (Fig. 4). For the experimental data a linear regression was obtained

$$D/\mathrm{cm}^{-1} = 32.7(4.8) - 151(10)\tau \quad (4)$$

with the correlation coefficient R^2 = 0.97. This is the first magnetostructural *D*-correlation applicable to pentacoordinate Ni(II) complexes.

Analogously, for the theoretical data a linear regression was obtained

$$D/\mathrm{cm}^{-1} = 33.1(7.1) - 150(16)\tau \quad (5)$$

with the correlation coefficient R^2 = 0.91. Both correlations obtained provided quantitatively almost the same values of parameters taking into account their standard errors, thus showing that both experimental and theoretical investigations are in harmony. Nevertheless, the linear correlation was studied within a somewhat limited range of τ values, and therefore enlarging the dataset could bring a new piece of knowledge. Previously reported Ni(II) compounds with τ values >0.6 have too different chromophores ($\{NiN_3X_2\}$ or $\{NiN_4X\}$, X = halide ligand)[12] from the presented series (and therefore ligand field strength) and this prevented us from involving them in our study.

Next, we focused on compound **6** in order to investigate the effect of the hydrogen bonds within the supramolecular dimer (Fig. 1) on the magnetic exchange in analogy with our previous work.[24] The DFT method was used in calculating the isotropic exchange coupling constant by using the broken-symmetry (BS) procedure at the B3LYP/def2-TZVP level of theory. The computation was performed for $[Ni(L5F)]_2$ dimer at the geometry as determined from the single-crystal X-ray analysis (Fig. 5),

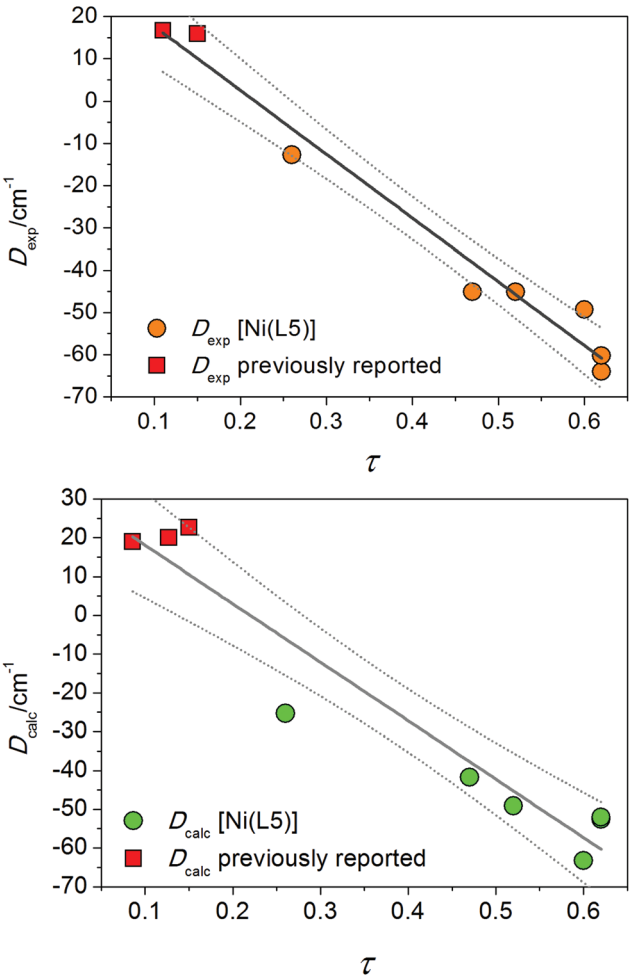

Fig. 4 A magneto-structural correlation, D *vs.* τ, for the experimental and theoretical data. The confidence interval with 95% is shown (dotted lines).

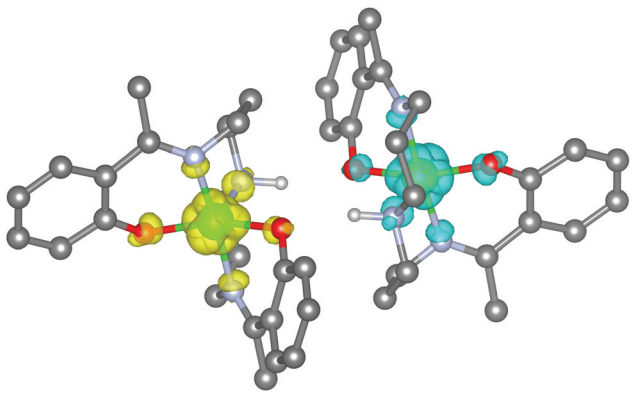

Fig. 5 The calculated isodensity surfaces of the broken symmetry spin state using B3LYP/def2-TZVP(-f) for the $[Ni(L5F)]_2$ dimer of **6**. Positive and negative spin densities are represented by yellow, and cyan surfaces, respectively, with the cut-off values of 0.01 e bohr^{-3}. Only hydrogen atoms within N–H···O hydrogen bonds are shown for clarity.

except for the positions of the hydrogen atoms which were optimised by using B3LYP/def2-TZVP(-f) and atom-pairwise dispersion correction by S. Grimme *et al.* (see details in the Experimental section). The analysis was based on the Heisenberg spin Hamiltonian,

$$\hat{H} = -J(\vec{S}_1 \cdot \vec{S}_2) \quad (6)$$

and energy difference between the broken-symmetry (BS) and high-spin (HS) spin states, $\Delta = E_{BS} - E_{HS}$, was used in evaluating J-values either by Ruiz approach[25]

$$J^{Ruiz} = \Delta/(2S_1S_2 + S_1) \quad (7)$$

or Yamaguchi approach[26]

$$J^{Yam} = 2\Delta/(\langle S^2\rangle_{HS} - \langle S^2\rangle_{BS}) \quad (8)$$

giving rise to $J^{Ruiz} = -0.60$ cm^{-1} and $J^{Yam} = -0.90$ cm^{-1}. The obtained data suggests a non-negligible value of the antiferromagnetic nature. We also tested whether the magnetic analysis can reveal such a small exchange under the condition that $|D| \gg |J|$. The calculations (Fig. S1 in ESI†) yielded $J = -0.28$ cm^{-1}, $D = -13.0$ cm^{-1}, $E/D = 0.15$, and $g = 2.259$, which are close to the parameters reported for a mononuclear unit. Such weak antiferromagnetic exchange is in agreement with the isothermal magnetization data, in which no inflection point was detected (Fig. S2 in ESI†).

Conclusions

We reported on a series of six pentacoordinate Ni(II) compounds with a focus on their structure and magnetism. The molecular structures of the presented complexes differ slightly in the shape of pentadentate Schiff base ligands, but also in the geometry of the coordination polyhedra. It was revealed that the τ parameter varies within the series from 0.26 (in **6**) to 0.62 (in **2** and **3**) and this means that the chromophore geometry of the presented compounds is between the square-pyramid and trigonal-bipyramid. It is expected that Ni(II) compounds having the chromophore geometry close to trigonal-bipyramid should possess large negative values of the axial ZFS parameter, while compounds with the chromophore geometry close to square-planar should possess positive D values. This was partially confirmed by our present study where the compounds with the largest τ values adopt also the largest negative D values (D(**2**) = −64.0 cm^{-1}, D(**3**) = −60.3 cm^{-1}) and the compound with the lowest τ adopts also the lowest D value (D(**6**) = −12.7 cm^{-1}). We did not observe positive D values in **1–6**, but it must be noted that the chromophore in **6**, as a border compound of the series, is still far from net square pyramid. Therefore, two previously reported compounds, [Ni(L3A)(L2)](ClO$_4$) (**7**) and [Ni(L3B)(L2)](ClO$_4$) (**8**) with the geometry of their coordination polyhedra close to square-planar (τ(**7**) = 0.09; τ(**8**) = 0.13), were involved in the discussion, which enabled us to derive the magneto-structural correlation for the axial ZFS parameter in the form D/cm^{-1} = 32.7(4.8) − 151(10) τ.

A similar correlation was obtained when *ab initio* values were involved, demonstrating that the magnetic analysis of the experimental data and theoretical calculations are in accordance. Despite large negative *D*-values, no out-of-phase AC susceptibility signal was detected for **1–5**, leaving the quest for the first pentacoordinate Ni(II) single-ion magnet still open.

Experimental

Synthesis

All reagents and solvents were purchased from commercial sources (Sigma Aldrich, Acros Organics) and used as received. Compounds **1–6** were prepared according to previously reported literature methods.[16] The experimental procedures for the preparation of **1–6** are similar and therefore, only the synthesis of **1** will be described in detail.

Synthesis of [Ni(L5A)]

2.48 g of $Ni(ac)_2{\cdot}4H_2O$ (0.01 mmol) was mixed with 3.84 g of 3-*tert*-butyl-2-hydroxy-5-methylbenzaldehyde (0.02 mmol) in 40 cm^3 of methanol. The solution was stirred for 30 min at room temperature. Then, the methanol solution of 3,3′-diamino-*N*-methyldipropylamine (0.01 mmol) was added dropwise and the pale-green solution turned dark green immediately. The solution was left stirring under heating (at boiling point of solution) for 30 min and then it was filtered through the paper filter and left to cool down and evaporate slowly. Single crystals (**1**) or microcrystalline material (**2–6**) were obtained and isolated after four days. Compounds **2**, **3**, **4** and **5** were recrystallized from dichloromethane–methanol solution (1 : 1, v/v). Compound **6** was recrystallized from toluene The recrystallized samples were used for elemental analysis and magnetic measurements.

Yields: 1, 82%; 2, 58%; 3, 64%; 4, 88%; 5, 83%; 6, 9%.

Elemental analysis. **1**, M_r = 550.4, $C_{31}H_{45}N_3NiO_2$, found: C, 67.4; H, 8.2; N, 7.4, requires C, 67.7; H, 8.2; N, 7.6%, **2**, M_r = 567.9, $C_{21}H_{23}Br_2N_3NiO_2$, found: C, 44.3; H, 4.2; N, 7.5, requires C, 44.4; H, 4.1; N, 7.4%, **3**, M_r = 661.9, $C_{21}H_{23}I_2N_3NiO_2$, found: C, 38.1; H, 3.3; N, 6.2, requires C, 38.1; H, 3.5; N, 6.4, **4**, M_r = 634.6, $C_{37}H_{57}N_3NiO_2$, found: C, 69.9; H, 9.3; N, 6.6, requires C, 70.0; H, 9.1; N, 6.6, **5**, M_r = 410.1, $C_{21}H_{25}N_3NiO_2$, found: C, 61.6; H, 6.3; N, 9.9, requires C, 61.5; H, 6.1; N, 10.3, **6**, M_r = 424.2, $C_{22}H_{27}N_3NiO_2$, found: C, 62.5; H, 6.4; N, 9.8, requires C, 62.3; H, 6.4; N, 9.9.

Equipment, measurements and software

Elemental analyses were performed using a CHNS Analyzer (ThermoFisher Scientific, FLASH 2000). The magnetic data were measured on powder samples pressed into pellets using a SQUID magnetometer (Quantum Design, MPMS-XL7) for **1–5** and PPMS system (Quantum Design, Dynacool) for **6**. The experimental data were corrected for the diamagnetism of the constituent atoms using Pascal constants.[27]

Single crystal X-ray diffraction data were collected using CCD diffractometer (Oxford Diffraction, Xcalibur2) with a Sapphire CCD detector installed at a fine-focus sealed tube (Mo-Kα radiation, λ = 0.71073 Å). All structures were solved by direct methods using SHELXS97[28] and SIR-92[29] incorporated into the WinGX program package.[30] For each structure its space group was checked by the ADSYMM procedure of the PLATON[31] software. All structures were refined using full-matrix least-squares on $F_o^2 - F_c^2$ with SHELXTL-97 with anisotropic displacement parameters for non-hydrogen atoms.[30] All hydrogen atoms were found in differential Fourier maps and their parameters were refined using a riding model with $U_{iso}(H)$ = 1.2 or 1.5U_{eq} (atom of attachment). All the crystal structures were visualized using the Mercury software.[32] Non-routine aspects of the structural refinement are as follows: aliphatic parts (carbon atoms) of the ligands in compounds **1**, **2**, **3** and **5** are disordered over two positions.

Theoretical methods. All theoretical calculations were performed with the ORCA 3.0 computational package.[33] The ZFS and *g* tensors were calculated by employing self-consistent field (SA-CASSCF) wave functions[34] complemented by N-electron valence second order perturbation theory (NEVPT2).[35] The active space of the CASSCF calculation was set to five d-orbitals of Ni(II) (CAS(8,5)). The ZFS parameters, based on dominant spin–orbit coupling contributions from excited states, were calculated through quasi-degenerate perturbation theory (QDPT),[36] in which approximations to the Breit–Pauli form of the spin–orbit coupling operator (SOMF approximation)[37] and the effective Hamiltonian theory[38] were utilized. The relativistic effects were included using zero order regular approximation (ZORA)[39] and the scalar relativistic contracted version of def2-TZVP(-f) basis functions[40] together with the def2-TZV/C auxiliary basis sets for correlation calculations utilizing the chain-of-spheres (RIJCOSX) approximation to exact exchange.[41] In the case of compound **6**, the DFT calculation of the *J*-value was done at the B3LYP/def2-TZVP(-f) level of theory. The hydrogen atom positions were optimized prior to calculation of the *J*-value using B3LYP/def2-TZVP(-f) and atom-pairwise dispersion correction to the DFT energy with the Becke–Johnson damping (D3BJ).[42] The spin densities were visualized with the program VESTA 3.[43]

Acknowledgements

We thank Marek Machata for preparation of the samples for SQUID measurements and Lucia Hanousková for help with synthesis. National Program of Sustainability I (LO1305) of the Ministry of Education, Youth and Sports of the Czech Republic, GAČR 13-27355P, VEGA 1/0522/14, VEGA 1/0233/12, and APVV-0014-11 are acknowledged for the financial support.

Notes and references

1 R. Boča, *Coord. Chem. Rev.*, 2004, **248**, 757–815.
2 F. Neese and D. A. Pantazis, *Faraday Discuss.*, 2011, **148**, 229–238.

3 N. Ishikawa, M. Sugita, T. Ishikawa, S.-Y. Koshihara and Y. Kaizu, *J. Am. Chem. Soc.*, 2003, **125**, 8694–8695.

4 (*a*) R. Ishikawa, R. Miyamoto, H. Nojiri, B. K. Breedlove and M. Yamashita, *Inorg. Chem.*, 2013, **52**, 8300–8302; (*b*) G. A. Craig, J. J. Marbey, S. Hill, O. Roubeau, S. Parsons and M. Murrie, *Inorg. Chem.*, 2014, **54**, 13–15; (*c*) J. Vallejo, A. Pascual-Álvarez, J. Cano, I. Castro, M. Julve, F. Lloret, J. Krzystek, G. De Munno, D. Armentano, W. Wernsdorfer, R. Ruiz-García and E. Pardo, *Angew. Chem., Int. Ed.*, 2013, **52**, 14075–14079.

5 (*a*) J. M. Zadrozny, D. J. Xiao, J. R. Long, M. Atanasov, F. Neese, F. Grandjean and G. J. Long, *Inorg. Chem.*, 2013, **52**, 13123–13131; (*b*) J. M. Zadrozny, D. J. Xiao, M. Atanasov, G. J. Long, F. Grandjean, F. Neese and J. R. Long, *Nat. Chem.*, 2013, **5**, 577–581.

6 (*a*) J. M. Zadrozny, M. Atanasov, A. M. Bryan, C.-Y. Lin, B. D. Rekken, P. P. Power, F. Neese and J. R. Long, *Chem. Sci.*, 2013, **4**, 125–138; (*b*) C. Mathonière, H.-J. Lin, D. Siretanu, R. Clérac and J. M. Smith, *J. Am. Chem. Soc.*, 2013, **135**, 19083–19086; (*c*) X. Feng, C. Mathonière, I.-R. Jeon, M. Rouzières, A. Ozarowski, M. L. Aubrey, M. I. Gonzalez, R. Clérac and J. R. Long, *J. Am. Chem. Soc.*, 2013, **135**, 15880–15884; (*d*) W. H. Harman, T. D. Harris, D. E. Freedman, H. Fong, A. Chang, J. D. Rinehart, A. Ozarowski, M. T. Sougrati, F. Grandjean, G. J. Long, J. R. Long and C. J. Chang, *J. Am. Chem. Soc.*, 2010, **132**, 18115–18126; (*e*) D. E. Freedman, W. H. Harman, T. D. Harris, G. J. Long, C. J. Chang and J. R. Long, *J. Am. Chem. Soc.*, 2010, **132**, 1224–1225; (*f*) D. Weismann, Y. Sun, Y. Lan, G. Wolmershäuser, A. K. Powell and H. Sitzmann, *Chem. – Eur. J.*, 2011, **17**, 4700–4704.

7 S. Mossin, B. L. Tran, D. Adhikari, M. Pink, F. W. Heinemann, J. Sutter, R. K. Szilagyi, K. Meyer and D. J. Mindiola, *J. Am. Chem. Soc.*, 2012, **134**, 13651–13661.

8 (*a*) T. Jurca, A. Farghal, P.-H. Lin, I. Korobkov, M. Murugesu and D. S. Richeson, *J. Am. Chem. Soc.*, 2011, **133**, 15814–15817; (*b*) N. Nedelko, A. Kornowicz, I. Justyniak, P. Aleshkevych, D. Prochowicz, P. Krupiński, O. Dorosh, A. Ślawska-Waniewska and J. Lewiński, *Inorg. Chem.*, 2014, **53**, 12870–12876; (*c*) R. Ruamps, L. J. Batchelor, R. Guillot, G. Zakhia, A.-L. Barra, W. Wernsdorfer, N. Guihery and T. Mallah, *Chem. Sci.*, 2014, **5**, 3418–3424; (*d*) X.-C. Huang, C. Zhou, D. Shao and X.-Y. Wang, *Inorg. Chem.*, 2014, **53**, 12671–12673; (*e*) R. Boča, J. Miklovič and J. Titiš, *Inorg. Chem.*, 2014, **53**, 2367–2369; (*f*) A. Eichhöfer, Y. Lan, V. Mereacre, T. Bodenstein and F. Weigend, *Inorg. Chem.*, 2014, **53**, 1962–1974; (*g*) D. M. Pinero Cruz, D. N. Woodruff, I.-R. Jeon, I. Bhowmick, M. Secu, E. A. Hillard, P. Dechambenoit and R. Clerac, *New J. Chem.*, 2014, **38**, 3443–3448; (*h*) V. Chandrasekhar, A. Dey, A. J. Mota and E. Colacio, *Inorg. Chem.*, 2013, **52**, 4554–4561; (*i*) Y.-Y. Zhu, C. Cui, Y.-Q. Zhang, J.-H. Jia, X. Guo, C. Gao, K. Qian, S.-D. Jiang, B.-W. Wang, Z.-M. Wang and S. Gao, *Chem. Sci.*, 2013, **4**, 1802–1806; (*j*) D.-K. Cao, J.-Q. Feng, M. Ren, Y.-W. Gu, Y. Song and M. D. Ward, *Chem. Commun.*, 2013, **49**, 8863–8865; (*k*) J. Vallejo, I. Castro, R. Ruiz-García, J. Cano, M. Julve, F. Lloret, G. De Munno, W. Wernsdorfer and E. Pardo, *J. Am. Chem. Soc.*, 2012, **134**, 15704–15707; (*l*) J. M. Zadrozny, J. Liu, N. A. Piro, C. J. Chang, S. Hill and J. R. Long, *Chem. Commun.*, 2012, **48**, 3927–3929; (*m*) J. M. Zadrozny and J. R. Long, *J. Am. Chem. Soc.*, 2011, **133**, 20732–20734; (*n*) R. Herchel, L. Váhovská, I. Potočňák and Z. Trávníček, *Inorg. Chem.*, 2014, **53**, 5896–5898.

9 R. C. Poulten, M. J. Page, A. G. Algarra, J. J. Le Roy, I. López, E. Carter, A. Llobet, S. A. Macgregor, M. F. Mahon, D. M. Murphy, M. Murugesu and M. K. Whittlesey, *J. Am. Chem. Soc.*, 2013, **135**, 13640–13643.

10 (*a*) R. Boča and J. Titiš, in *Coordination Chemistry Research Progress*, Nova Science Publishers, New York, 2008, p. 247; (*b*) J. Titiš and R. Boča, *Inorg. Chem.*, 2010, **49**, 3971; (*c*) A. Packová, J. Miklovič, J. Titiš, M. Koman and R. Boča, *Inorg. Chem. Commun.*, 2013, **32**, 9; (*d*) J. Miklovič, A. Packová, P. Segľa, J. Titiš, M. Koman, J. Moncoľ, R. Boča, V. Jorík, H. Krekuzska and D. Valigura, *Inorg. Chim. Acta*, 2015, **429**, 73–80; (*e*) J. Titiš and R. Boča, *Inorg. Chem.*, 2011, **50**, 11838; (*f*) J. Miklovič, R. Boča and J. Titiš, submitted to *Dalton Trans.*

11 C. Rajnák, J. Titiš, I. Šalitroš, R. Boča, O. Fuhr and M. Ruben, *Polyhedron*, 2013, **65**, 122.

12 (*a*) R. Ruamps, R. Maurice, L. Batchelor, M. Boggio-Pasqua, R. Guillot, A. L. Barra, J. Liu, E.-E. Bendeif, S. Pillet, S. Hill, T. Mallah and N. Guihéry, *J. Am. Chem. Soc.*, 2013, **135**, 3017–3026; (*b*) J.-N. Rebilly, G. Charron, E. Rivière, R. Guillot, A.-L. Barra, M. D. Serrano, J. van Slageren and T. Mallah, *Chem. – Eur. J.*, 2008, **14**, 1169–1177.

13 M. Gruden-Pavlovic, M. Peric, M. Zlatar and P. Garcia-Fernandez, *Chem. Sci.*, 2014, **5**, 1453–1462.

14 (*a*) R. Cini, *Inorg. Chim. Acta*, 1983, **73**, 146–152; (*b*) R. Herchel and R. Boča, *Dalton Trans.*, 2005, 1352–1353; (*c*) R. Boča, H. Elias, W. Haase, M. Huber, R. Klement, L. Muller, H. Paulus, I. Svoboda and M. Valko, *Inorg. Chim. Acta*, 1998, **278**, 127–135.

15 M. Franks, A. Gadzhieva, L. Ghandhi, D. Murrell, A. J. Blake, E. S. Davies, W. Lewis, F. Moro, J. McMaster and M. Schröder, *Inorg. Chem.*, 2013, **52**, 660–670.

16 I. Bertini, L. Sacconi and G. P. Speroni, *Inorg. Chem.*, 1972, **11**, 1323–1326.

17 M. Amirnasr, K. J. Schenk, S. Meghdadi and M. Morshedi, *Polyhedron*, 2006, **25**, 671–677.

18 M. Seleborg, S. L. Holt and B. Post, *Inorg. Chem.*, 1971, **10**, 1501–1504.

19 (*a*) Cambridge Crystallographic Database (CSD, ver. 5.35, May 2014 update). (*b*) F. H. Allen, *Acta Crystallogr., Sect. B: Struct. Sci.*, 2002, **58**, 380–388.

20 A. W. Addison, T. N. Rao, J. Reedijk, J. Vanrijn and G. C. Verschoor, *J. Chem. Soc., Dalton Trans.*, 1984, 1349–1356.

21 I. Nemec, R. Boča, M. Gembický, L. Dlháň, R. Herchel and F. Renz, *Inorg. Chim. Acta*, 2009, **362**, 4754–4759.

22 The standard deviations were calculated as $\sigma_i = (P_{ii}^{-1} \cdot S/(N-k))^{-1/2}$, where $P_{ij} = \sum(\delta\mu_n/\delta a_i \cdot \delta\mu_n/\delta a_j)$ and $S = \sum(\mu_n - \mu_n^{exp})^2$ with $n = 1$ to N; a_i and a_j are fitted parameters, N is number of experimental points (sum of temperature and field dependent data), μ_n and μ_n^{exp} are the calculated and experimental effective magnetic moments for given temperature and magnetic field. The σ_i was then multiplied by Student's $t_{95\%}$ to provide confidence limits with 95% probabilities listed in the text.
23 J.-P. Costes, R. Maurice and L. Vendier, *Chem. – Eur. J.*, 2012, **18**, 4031–4040.
24 I. Nemec, R. Herchel, T. Šilha and Z. Trávníček, *Dalton Trans.*, 2014, **43**, 15602–15616.
25 (*a*) E. Ruiz, J. Cano, S. Alvarez and P. Alemany, *J. Comput. Chem.*, 1999, **20**, 1391–1400; (*b*) E. Ruiz, A. Rodríguez-Fortea, J. Cano, S. Alvarez and P. Alemany, *J. Comput. Chem.*, 2003, **24**, 982–989.
26 (*a*) K. Yamaguchi, Y. Takahara and T. Fueno, in *Applied Quantum Chemistry*, ed. V. H. Smith, Reidel, Dordrecht, 1986, p. 155; (*b*) T. Soda, Y. Kitagawa, T. Onishi, Y. Takano, Y. Shigeta, H. Nagao, Y. Yoshioka and K. Yamaguchi, *Chem. Phys. Lett.*, 2000, **319**, 223.
27 R. Boča, *A Handbook of Magnetochemical Formulae*, Elsevier, Amsterdam, 2012.
28 G. M. Sheldrick, *Acta Crystallogr., Sect. A: Found. Crystallogr.*, 2008, **64**, 112.
29 A. Altomare, G. Cascarano, C. Giacovazzo, A. Guagliardi, M. C. Burla, G. Polidori and M. Camalli, *J. Appl. Crystallogr.*, 1994, **27**, 435.
30 L. J. Farrugia, *J. Appl. Crystallogr.*, 1999, **32**, 837.
31 (*a*) A. L. Speck, *PLATON, a multipurpose crystallographic tool*, Utrecht University, Utrecht, The Netherlands, 2001; (*b*) Y. Le Page, MISSYM1.1 – a flexible new release, *J. Appl. Crystallogr.*, 1988, **21**, 983.
32 C. F. Macrae, P. R. Edgington, P. McCabe, E. Pidcock, G. P. Shields, R. Taylor, M. Towler and J. van de Streek, *J. Appl. Crystallogr.*, 2006, **39**, 453.
33 F. Neese, *WIREs: Comput. Mol. Sci.*, 2012, **2**, 73–78.
34 P. A. Malmqvist and B. O. Roos, *Chem. Phys. Lett.*, 1989, **155**, 189–194.
35 (*a*) C. Angeli, R. Cimiraglia, S. Evangelisti, T. Leininger and J. P. Malrieu, *J. Chem. Phys.*, 2001, **114**, 10252–10264; (*b*) C. Angeli, R. Cimiraglia and J. P. Malrieu, *Chem. Phys. Lett.*, 2001, **350**, 297–305; (*c*) C. Angeli, R. Cimiraglia and J. P. Malrieu, *J. Chem. Phys.*, 2002, **117**, 9138–9153; (*d*) C. Angeli, S. Borini, M. Cestari and R. Cimiraglia, *J. Chem. Phys.*, 2004, **121**, 4043–4049; (*e*) C. Angeli, B. Bories, A. Cavallini and R. Cimiraglia, *J. Chem. Phys.*, 2006, **124**, 054108.
36 D. Ganyushin and F. Neese, *J. Chem. Phys.*, 2006, **125**, 024103.
37 F. Neese, *J. Chem. Phys.*, 2005, **122**, 034107.
38 R. Maurice, R. Bastardis, C. de Graaf, N. Suaud, T. Mallah and N. Guihéry, *J. Chem. Theory Comput.*, 2009, **5**, 2977–2984.
39 (*a*) E. Vanlenthe, E. J. Baerends and J. G. Snijders, *J. Chem. Phys.*, 1993, **99**, 4597–4610; (*b*) C. van Wullen, *J. Chem. Phys.*, 1998, **109**, 392–399.
40 D. A. Pantazis, X.-Y. Chen, C. R. Landis and F. Neese, *J. Chem. Theory Comput.*, 2008, **4**, 908–919.
41 F. Neese, F. Wennmohs, A. Hansen and U. Becker, *Chem. Phys.*, 2009, **356**, 98–109.
42 (*a*) S. Grimme, J. Antony, S. Ehrlich and H. Krieg, *J. Comput. Chem.*, 2010, **132**, 154104; (*b*) S. Grimme, S. Ehrlich and L. Goerigk, *J. Comput. Chem.*, 2011, **32**, 1456–1465.
43 K. Momma and F. Izumi, *J. Appl. Crystallogr.*, 2011, **44**, 1272–1276.